Semiquantitative Analysis of the Thermal Degradation of Polypropylene

Tomoyuki Ishikawa,[1] Tomohiro Ohkawa,[1] Masaaki Suzuki,[1] Toshiaki Tsuchiya,[2] Kunihiko Takeda[3]

[1]*Department of Materials Science and Engineering, Graduate School of Engineering, Shibaura Institute of Technology, 3-9-14 Shibaura, Minato-ku, Tokyo 108-8548, Japan*
[2]*Research Organization for Advanced Engineering, Shibaura Institute of Technology, Tokyo, Japan*
[3]*Department of Materials Science and Engineering, Graduate School of Engineering, Nagoya University, Furo-cho, Chikusa-ku 464-0083, Japan*

Received 11 March 2002; accepted 27 June 2002

ABSTRACT: The pyrolysis product distributions of polypropylene (PP) were observed, and the experimental data were semiquantitatively analyzed by computer simulation with the Molic mouse method. Studies by many researchers on PP decomposition and experimental results achieved in this study were examined. The product distributions were classified into three types of hydrocarbon products: $3n$, $3n + 1$, and $3n + 2$ (n = monomer unit). The ratio showed the characteristic tendency, and the thermal degradation of PP appeared to include very complicated scission paths. The Molic mouse method, which was applied to the analysis of the thermal rearrangement and decomposition of poly(phenylene ether), was used to simulate the experimental results. After several steps by which the proper model was constructed, the scission probabilities to generate $2 \times 3n$, $3n + 1$ and $3n + 2$, $3n$ and $3n + 1$, $3n$ and $3n + 2$, C9, and C15 hydrocarbons were successfully calculated to be 0.25, 0.67, 0.47, 0.35, 1.0, and 0.33, respectively. This meant that the scission process of PP was very simple except for the C9 and C15 generation paths, for which the cyclic compounds were stable intermediates. © 2003 Wiley Periodicals, Inc. J Appl Polym Sci 88: 1465–1472, 2003

Key words: poly(propylene) (PP); degradation; simulations; flame retardance

INTRODUCTION

The thermal degradation of polypropylene (PP) has been studied from different points of view. In the early years, when researchers were simply interested in the polymer degradation itself with respect to the assignment of the scission products, the activation energy and fundamental mechanism were investigated and reported.[1–3] Thermogravimetric analysis and pyrolysis–gas chromatography/mass spectrometry (Py–GC/MS) were often used to observe residues and to determine other basic information concerning the thermal degradation.[4–6] Research was gradually developed for various purposes such as the kinetics, individual reactions, and intermediate assignments.[7,8] Researches interested in actual usage have made headway in stabilizing the production or processing of PP, improving its deterioration and flame retardancy for its service time and studying its recovery from waste plastics.[9,10]

Despite the previously cited works, a detailed and total description of PP degradation has not been achieved yet. The plural steric structures of PP are one reason, and the different conditions adopted by every researcher are another reason. Propene and butene have been reported as the major degradation products for both isotactic PP and atactic PP at high temperatures. For example, relatively smaller hydrocarbons such as C3, C4, and C6 were recovered by Sawaguchi et al.[7] at high temperatures and long residence times; the primary decomposition products were supposed to be waxlike materials, and they subsequently decomposed into smaller hydrocarbons in the reaction vessel or gaseous phase.

In other words, there is little value in a direct comparison of scission products because different conditions, samples, and pyrolyzers produce different data. This study was undertaken to supply data for a basic study on thermal degradation, scission product distribution, and semiquantitative analysis by computer simulation.

EXPERIMENTAL AND SIMULATION

Experimental

The isotactic PP was manufactured by Chisso Co., Ltd. (Tokyo, Japan) [Chisso Polypro K4017; density = 0.90 kg/m^3, melt-flow rate (used as a flow index of the melted polymer) = 7.5].

Correspondence to: K. Takeda (nagoyatakeda@numse.nagoya-u.ac.jp).

Contract grant sponsor: New Energy and Industrial Technology Development Organization.

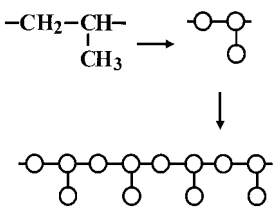

Figure 1 Molic mouse model of PP.

Thermogravimetric analysis (TGA-50, Shimadzu Co., Ltd., Tokyo, Japan) was used at a heating rate of 40°C/min from room temperature to 800°C. Py–GC (Shimadzu GC-17A equipped with a Nippon Bunseki Curie point pyrolyzer) was used for the thermal degradation. The separation column was a phenylmethylsiloxane capillary column (0.25×10^{-3} m in diameter and 30 m long) coated by a 5% liquid phase. The flow rate of the carrier gas (He) was 1×10^{-3} dm^3/min. The temperatures of the GC injector and the detector were 280 and 200°C, respectively.

A mass spectrometer (GCMS-QP5000, Shimadzu) was used for the assignment of the scission products. The interface temperature between the pyrolyzer and the gas chromatograph was 280°C; a 27-m-long capillary column was mounted, and the linear velocity of the helium gas was 26.4 cm/s. The minimum and maximum mass numbers were 45 and 500, respectively.

Simulation

The unit, which could be a simply represented polymer, had to be depicted with the Molic mouse method. The unit of PP was much simpler than the units of other polymers,[11] as shown in Figure 1.

The scission routes of PP could be postulated from the degradation mechanism described in previous publications and the experimental data obtained in this study. The polymer chain of the $3n$ type, shown later in Table II, decomposed in two ways. One generated two $3n$-type hydrocarbons with the probability of A, and the other generated $3n + 1$-type and $3n + 2$-type hydrocarbons with the probability of B, as depicted in Figure 2. Subsequently, the $3n + 1$-type and $3n + 2$-type chains degraded into $3n$ and $3n + 1$ hydrocarbons and $3n$ and $3n + 2$ hydrocarbons with the probabilities of C and D, respectively.

An entire block diagram and a flow sheet are illustrated in Figure 3. The initial conditions and parameters necessary for the simulation were set during the initial procedure in the program. The molecular weight (the unit number), steric structure (the special restriction or scission), and other necessary conditions were completed during the procedure. The model scissions were achieved in the following loop in which the calculated values were immediately compared with corresponding experimental values. The entire diagram and procedure are shown in Figure 3.

The simulation procedure in Figure 3 is much simpler than those of the simulation programs often applied for the simulation of polymer degradation. This is a characteristic of the Molic mouse method. In particular, the procedure is simplest in Molic mouse programs for other polymers because the monomer and polymer structure are simple and there are few reactions except for direct chain scission, such as rearrangement, oxidation, and dehydrogenation, that should be taken into consideration.

RESULTS AND DISCUSSION

Fundamental data and classification of scission products

The thermal degradation of PP has intensively been researched from various points of view, including

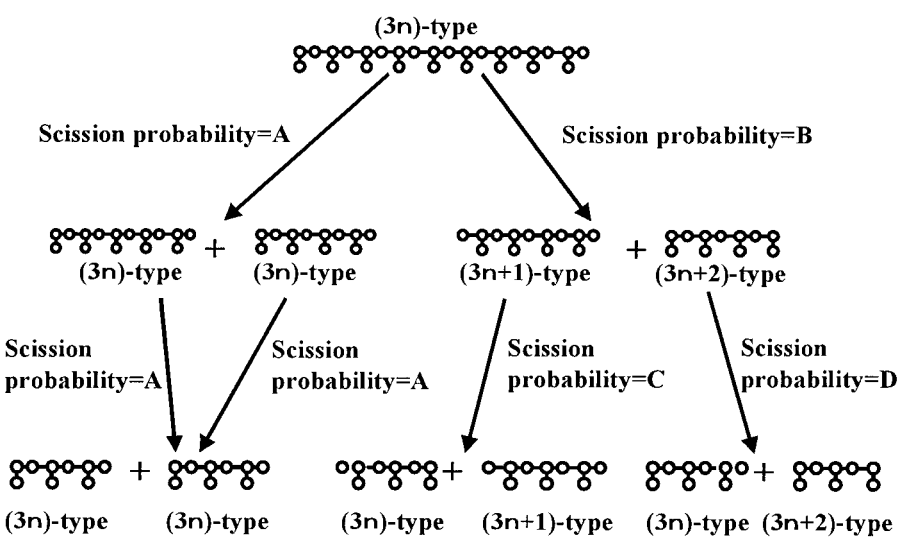

Figure 2 Scission routes and probabilities.

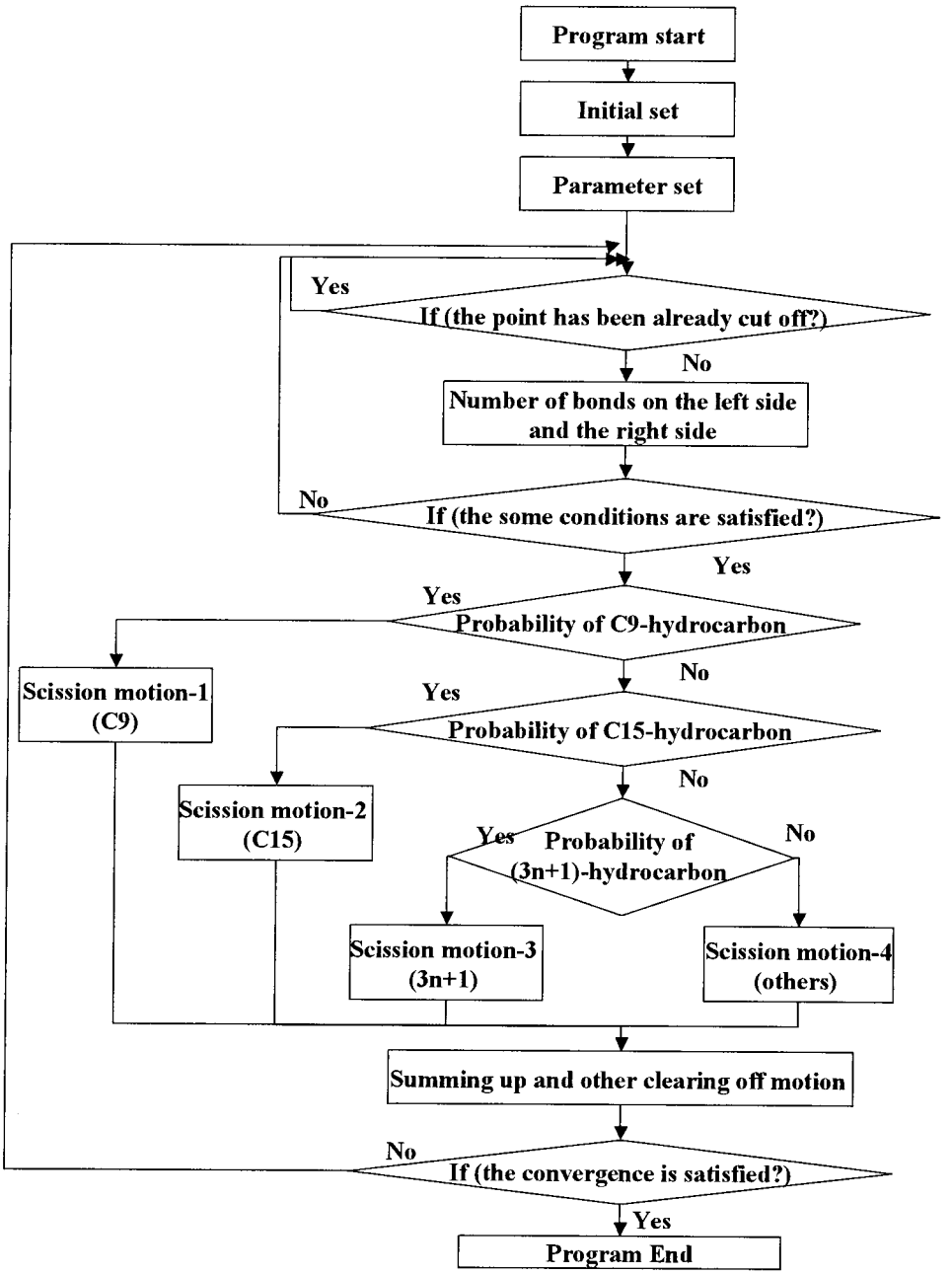

Figure 3 Main flow chart for the Molic mouse simulation of PP thermal degradation.

thermal, photo, photothermal, and mechanical degradation. Typical data for the thermal degradation can be found on the product spectrum for PP Py under various conditions. Tsuge and Ohtani[12] measured the degradation phenomena in almost every kind of polymer, and they drew charts and showed references in their book. They assigned the second largest peak of PP degradation to C15; other researchers chose C14 compounds. Murata and Makino[13] attributed this inconsistency to the close boiling points of their isomers. In this work, we assigned the peak to C15 as Tsuge and Ohtani did. Murata and Makino also reported spectra of small hydrocarbons, which are listed in Table I.

Although olefins were major products (see Table I), paraffins were also observed in the scission products. Smaller hydrocarbons were also recovered and reported by Sawaguchi et al.[7] The primary decomposition products were thought to be waxlike materials, and they successively decomposed into smaller hydrocarbons in the reaction vessel.

However, the results obtained by the different groups did not agree. One of the reasons was the different designs of their Py reactors. Another rea-

TABLE I
Product Spectrum obtained by Murata and Makino[13]

		Degradation temperature	
n	Component	380°C (mol %)	410°C (mol %)
0	H_2	1.5	0.9
1	CH_4	12.0	7.8
2	C_2H_4	0.7	0.7
2	C_2H_6	11.4	9.0
3	C_3H_6	37.0	37.9
3	C_3H_8	7.4	4.9
4	l-C_4H_8	0.0	0.0
4	i-C_4H_8	28.6	37.5
4	n-C_4H_8	0.8	0.7
5	C_5	0.6	0.6
n	$\bar{M}_n$	41.3	44.0

$\bar{M}_n$: Average molecular weight of volatile scission products.

son was that the PP samples themselves were different. This implies that a discussion on the degradation process and mechanism is more important than listing the scission products in the individual cases.

Before the analysis, a typical saturated hydrocarbon series of the scission products was classified (Table II). Three types of hydrocarbon were recognized. The first was the $3n$ type, the carbon numbers of which were 6, 9, 12, and so forth. The second was the $3n + 1$ type, the carbon numbers of which were 7, 11, 13, and so forth; it had methyl groups at both ends. The third type was the $3n + 2$ type, the carbon numbers of which were 5, 8, 11, and so forth. Those scission products existed as olefins and diolefins, which are shown in Table III with a carbon number of 6.

As shown in Table III, two types of olefins were assigned: 2-methyl-1-pentene and 4-methyl-2-pentene. The thermogravimetric analysis could show the entire profile of the thermal decomposition of PP, as depicted in Figure 4. The decomposition began at 380°C, and it was finished at 520°C. The residue at 600°C was very small, and this is one of the characteristics of olefin polymers.

Scission product analysis

The scission products from C4 to C40 are listed in Table IV, in which a clear tendency can be seen. Paraffins were hardly observed in the scission products by Py–GC/MS. The peaks that originated in $3n$-type and $3n + 2$-type diolefins were too small for the quantitative calculation of the amounts. However, olefins and diolefins were observed in $3n + 1$-type products, and the ratio of diolefins to olefins increased with an increasing carbon number. However, $3n + 2$-type products decreased, and those greater than C17 were not detected.

In summary, four types of hydrocarbons from nine types might be recognized, as listed in Table V. The olefins were of all types. However, the diolefins were only of the $3n + 1$ type.

The ratio of carbons on the main chain and side chain was theoretically expected to be 2:1 for $3n$-type products, n:$n + 2$ for $3n + 1$ products, and $n + 1$:$n + 2$ for $3n + 2$ products. The amount of hydrogen was smaller than that expected from the structure of the scission; products for paraffins were not observed. As shown in Table I, the paraffins seemed to be rich in smaller hydrocarbons, and hydrogen gas should be considered for taking the hydrogen mass balance.

The distributions of the three types of products are plotted in Figure 5. Low molecular weight hydrocarbons of $3n$ and $3n + 2$ scission products were more numerous than higher molecular weight ones. The amounts of C9 and C15 scission products were much higher than those of other products. Sakata et al.[14] observed the same pattern, and Tsuchiya and Murata and their coworkers[15,16] assigned C9 to 2,4-dimethyl-1-heptane (propylene trimer). Schooten and Wijga[17] got the same results with Fourier transform infrared spectroscopy.

TABLE II
Typical Saturated Hydrocarbon Series of PP Scission Products

	Carbon number			
	4	5	6	7
Structure	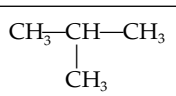	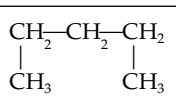	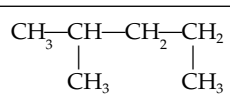	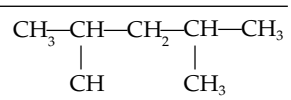

TABLE III
Chemical Structure of $3n$-Type Products for Six-Carbon Compounds

	Parafin	Olefin		Diolefin
Structure	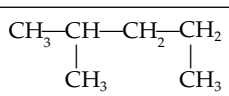	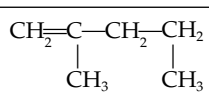	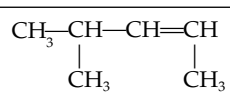	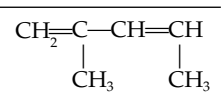

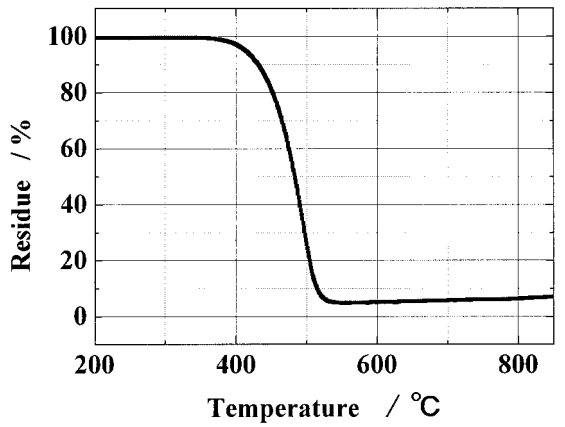

Figure 4 Thermogravimetric analysis of PP.

The ratio of olefins to diolefins in Figure 6 is also interesting. Diolefins increased as the carbon number increased, and the ratio of saturated carbon to unsaturated carbon was calculated to be 1.00:1.70.

To clarify the tendencies shown in Figures 5 and 6, many researchers have studied the organic reactions and kinetics of PP. The earliest works showed that the degradation temperatures of various polymers were proportional to the bond energies for many polymers.[18] The temperature of PP was 450°C because of a bond energy of 348.6 kJ/mol. Studies on radical decomposition reactions elucidated four individual steps: (1) the elimination of tertiary hydrogen, (2) the generation of radicals, (3) α scission or β scission, and (4) two types of radicals (see Fig. 7).[19] α scission is much smaller than β scission. It is thought to cause the larger amount of the $3n$ type in comparison with the amounts of the $3n + 1$ and $3n + 2$ types in the volatile products.

TABLE V
Scission Products by Formally Technical Procedure

	Types		
Type	$3n$	$3n + 1$	$3n + 2$
Paraffin	x	x	x
Olefin	○*	○	○
Diolefin	x	○	x

○ = assigned from experimental data; x = not recognized in these experiments.

However, the C9 product (mainly 2,4-dimethyl-1-heptene) was thought to be generated by the route shown in Figure 8, in which the para C6 ring that forms initially for it is relatively stable. Subsequently, the radical transfers on the fifth carbon at the left end, and it decomposes with β scission. This route is called *backbiting*.[20]

After both β scissions, the C5 product immediately decomposes into lower molecular weight compounds. This is the reason that the concentration of the C9 hydrocarbon is much higher than that of other hydrocarbons, and this scheme does not lack consistency from the viewpoint of organic chemistry.

Semiquantitative simulation by the molic mouse method

Although the previous discussions contributed to our understanding of the tendency of the scission products, the plots in Figures 5 and 6 could not be explained quantitatively. Therefore, the Molic mouse method, an adequate computer simulation technique for analyzing polymer degradation, was applied to PP degradation. A detailed description and the simula-

TABLE IV
Distribution of Recovered Scission Hydrocarbons

Number of carbons	Parafin	Olefin	Diolefin	Total (%)	Number of carbons	Parafin	Olelin	Diolefin	Total (%)
C4	—	1.47	—	1.47	C23	—	—	—	0.00
C5	—	3.31	—	3.31	C24	—	1.69	—	1.69
C6	—	4.54	—	4.54	C25	—	1.01	2.04	3.05
C7	—	3.52	0.68	4.21	C26	—	—	—	0.00
C8	—	1.29	—	1.29	C27	—	1.34	—	1.34
C9	—	21.88	—	21.88	C28	—	1.08	2.71	3.79
C10	—	2.05	0.97	3.02	C29	—	—	—	0.00
C11	—	0.94	—	0.94	C30	—	1.59	—	1.59
C12	—	2.82	—	2.82	C31	—	1.10	3.01	4.11
C13	—	1.38	1.15	2.54	C32	—	—	—	0.00
C14	—	0.50	—	0.50	C33	—	1.64	—	1.64
C15	—	5.33	—	5.33	C34	—	1.21	3.40	4.61
C16	—	1.48	1.53	3.01	C35	—	—	—	0.00
C17	—	—	—	0.00	C36	—	1.89	—	1.89
C18	—	2.33	—	2.33	C37	—	1.37	3.67	5.04
C19	—	1.20	1.71	2.91	C38	—	—	—	0.00
C20	—	—	—	0.00	C39	—	1.42	—	1.42
C21	—	2.14	—	2.14	C40	—	1.09	2.94	4.03
C22	—	1.29	2.25	3.55					

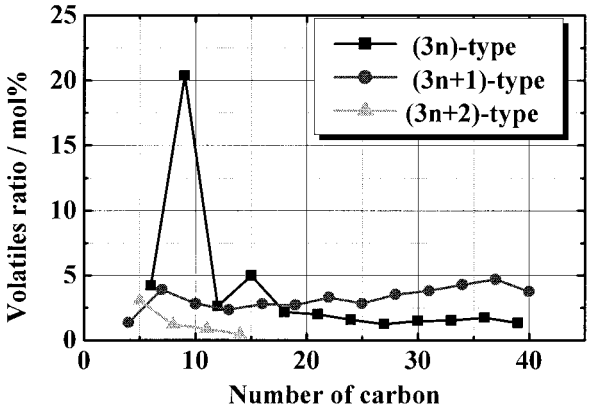

Figure 5 Distribution of the PP scission products at 550°C.

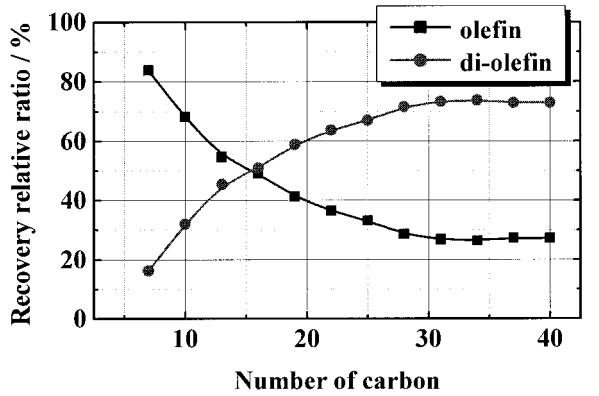

Figure 6 Distribution of the olefin and diolefin scission products.

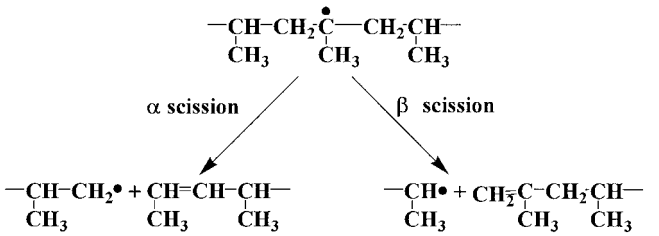

Figure 7 Fundamental scission mechanism of the PP main chain by thermal degradation.

tion procedure for this method can be found in a previous article.[21]

The simulation was achieved under the simplest assumption: all bonds of the PP main chain decompose with equal possibility, whereas the volatile products inhaled in GC do not decompose there. Figure 9 shows the simulation results. Two clear tendencies could be obtained. One was that three types of hydrocarbons increased with a decreasing carbon number. The other was that the amount of the $3n$ type was twice as large as the amount of the $3n + 1$ and $3n + 2$ types. The latter was due to the double chances by which the $3n$ type was generated from the PP chains, as depicted in Figure 2. This means that one of the reasons that the larger amount of the $3n$ type was recovered in the experiments plotted in Figure 5 was not the contribution of the electron distribution on the carbons but instead the simple probability due to the inherent structure of PP.

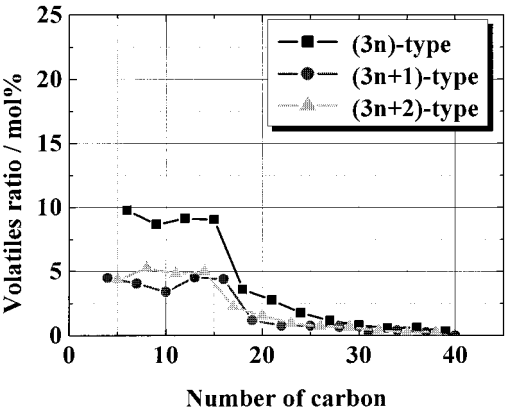

Figure 9 Simulation results obtained under the assumption that volatile scission products do not decompose in the gaseous phase (at 550°C).

Before the simulation was finished, the assumption that the volatile products did not decompose in the gaseous phase was not considered to be a special condition. However, the results showed a clear turning point between small and large hydrocarbons. These unexpected results were deduced by researchers and contributed to the simulation. Therefore, other simulations were performed under the assumption that the volatile products decomposed in the gaseous phase. The results are shown in Figure 10. The amount of small hydrocarbons increased in comparison with the results in Figure 9. This met our expectations and gave us a method for calculating the scission probability in the gaseous phase.

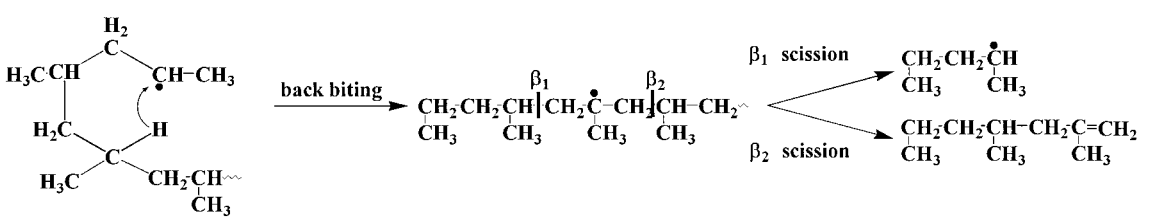

Figure 8 C6 structure before scission and β_i positions.

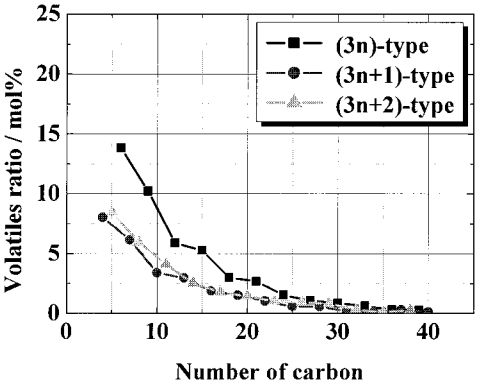

Figure 10 Simulation results obtained under the assumption of perfectly random scission.

The third point that should be checked before whole fitting is the treatment of C9 and C15. Figure 11 shows the results of the simulation in which the scission probabilities of C9 and C15 were studied, and it shows that the characteristic tendency could be fit by a change in the scission probability of both products without any consideration of other parameters. However, it was unexpected that the amount of the $3n + 1$-type higher hydrocarbon would be near zero. This was caused by precedence being taken over the scission of low molecular products.

Finally, the fitting to the experimental data was achieved. Satisfactory results could be obtained by well-designed Molic mouse simulation in almost every case. However, the discussion in progress is more important than that of the final result for our understanding of the phenomena.

Figure 12 presents the final plots of the simulation, and the scission probabilities are also listed in Table VI. The probability of generating the C9 product (P_D), which was the richest of all the hydrocarbons, was postulated to be 1.0. P_F (for C15) was 0.33. This means that the scission probability of generating C15 was a third of that of C9. P_A, P_B, P_C, and P_D, corresponding to the scission routes shown in Figure 2, were 0.25,

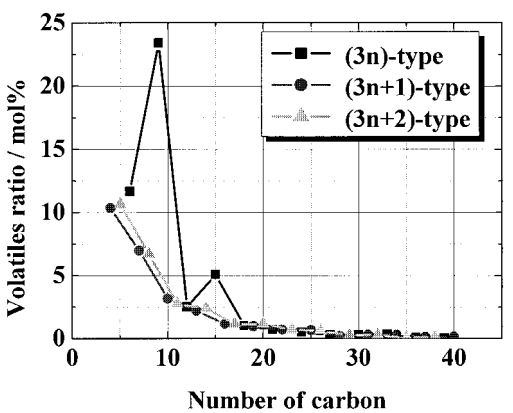

Figure 11 One set of simulation results fitting C9 and C15.

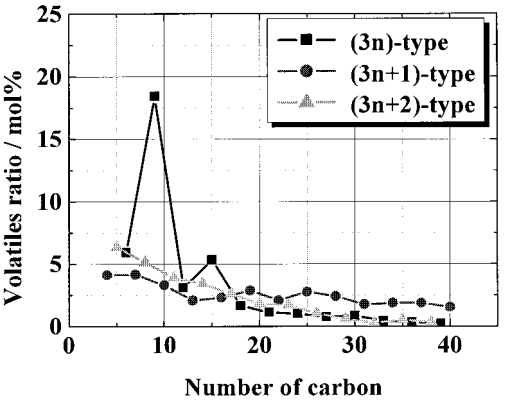

Figure 12 Distribution based on all the knowledge of the experiments and theory.

TABLE VI
Scission Probabilities of PP Thermal decomposition

	Scission probability					
	P_A	P_B	P_C	P_D	P_E	P_F
Figure 9 assumption	1.00	1.00	1.00	1.00	1.00	1.00
Figure 10 assumption	1.00	1.00	1.00	1.00	1.00	1.00
Figure 11 assumption	0.20	0.40	0.20	0.20	1.00	0.70
Final fitting	0.25	0.67	0.47	0.35	1.00	0.33

0.67, 0.47, and 0.35, respectively. The probability of P_B was 2.68 times greater than that of P_A. This seemed to be inconsistent with the experimental results, in which $3n$-type hydrocarbons were richer than $3n + 1$ and $3n + 2$ types.

As mentioned previously, there has much research into PP thermal decomposition. Excellent analytical work and studies on organic reactions are known. The higher probabilities of generating C9 and C15 are due to more stabilized cyclic compounds as intermediates. However, the decomposition process seems to be very simple on the basis of the experiments, simulations, and articles already published. The number of paths for generating the $3n$ product is four times that of the other two paths. This causes P_B to be 0.67 and P_A to be 0.25. P_C and P_D are almost the same, and the number of the paths is 1.0, as shown in Figure 2. In other words, simple and random scission occurs almost perfectly during the thermal decomposition of PP, although the four kinds of scission probabilities (P_A to P_D) are apparently different.

The authors thank S. Takayama (Asahi Chemicals Co., Ltd.) for his advice on flame retardancy and K. Murata (Mitsui Zosen Industrial Co., Ltd.) for his proposal concerning PP degradation data.

References

1. Madorsky, S. L.; Straus, S. J Res Natl Bur Stand 1954, 53, 361.
2. Wall, L. A.; Straus, S. J Polym Sci 1960, 44, 313.

3. Coverhill, A. R.; Taylor, G. W. Polymer 1965, 16, 193.
4. Seeger, M.; Cantow, H. J. Makromol Chem 1975, 176, 1411.
5. Seeger, M.; Ritter, R. J. J Polym Sci 1975, 176, 1411.
6. Kiang, J. K. Y.; Uden, P. C.; Chien, J. C. W. Polym Degrad Stab 1980, 2, 113.
7. Sawaguchi, T.; Suzuki, K.; Kuroki, T.; Ikemura, T. J Appl Polym Sci 1981, 26, 1267.
8. Bockhorn, H.; Hornung, A.; Hornung, U.; Schawaller, D. J Anal Appl Pyrolysis 1999, 48, 93.
9. Sodero, S. F.; Berruti, L. Chemie Ingenieur Technik 1974, 46, 579.
10. Westerhout, R. W. J.; Kuipers, J. A. M.; van Swaaij, W. P. M. Ind Eng Chem Res 1998, 37, 841.
11. Nemoto, T.; Yonezawa, S.; Soda, T.; Takeda, K. Polym Degrad Stab 2000, 69, 191.
12. Tsuge, S.; Ohtani, H. Fundamental Data of Polymer Thermal Degradation by Gas Chromatography; Techno System, Tokyo, Japan: 1989; p 312.
13. Murata, K.; Makino, T. J Chem Soc Jpn 1975, No. 1, 192.
14. Sakata, Y.; Uddin, M. A.; Muto, A. J Anal Appl Pyrolysis 1999, 51, 135.
15. Tsuchiya, Y.; Sumi, K. J Polym Sci Part A-1: Polym Chem 1969, 7, 1600.
16. Murata, K.; Makino, T. J Chem Soc Jpn 1975, No. 1, 195.
17. Schooten, J. V.; Wijga, P. W. O. High Temp Resist Therm Degrad Polym 1961, 13, 439.
18. Mortimer, C. T. Reaction Heats and Bond Strengths; Pergamon: Oxford, 1962.
19. Madorsky, S. L. Thermal Degradation of Organic Polymers; Interscience: New York, 1964.
20. Tsuchiya, Y.; Sumi, K. J Polym Sci Part A-1: Polym Chem 1969, 7, 1599.
21. Yonezawa, S.; Sohda, T.; Takeda, K. Polym Degrad Stab 2000, 69, 191.